adipocyte-specific culture medium, all cell lines accumulated lipid-rich vacuoles in their cytoplasm within 2 wk, which were made evident by Oil Red-O staining. In particular, the UE6E7T-3 cell line showed a greater adipogenetic ability among the four cell lines (Fig. 4*Ab*). In osteoblast induction medium for 2 wk, UCB408E6E7 TERT-33 cells showed a marked increase in alkaline phosphatase expression, a marker of osteoblast, compared with those in the three other cell lines (Fig. 4*Ad*). In addition, UBE6T-6 cells in neuron induction medium reduced proliferation and displayed marked changes in morphology from being a flat-polygonal shape to taking on the characteristic neuron-like shape in which the cells develop long branching processes. Moreover, in comparing the expression patterns of characteristic neural antigens, i.e., neurofilament, III-β-tubulin, before and after induction (28 d), the pseudo-neural shaped cells showed apparent increases in immunoreactivity to both antibodies (Fig. 4*Af, Ah*),

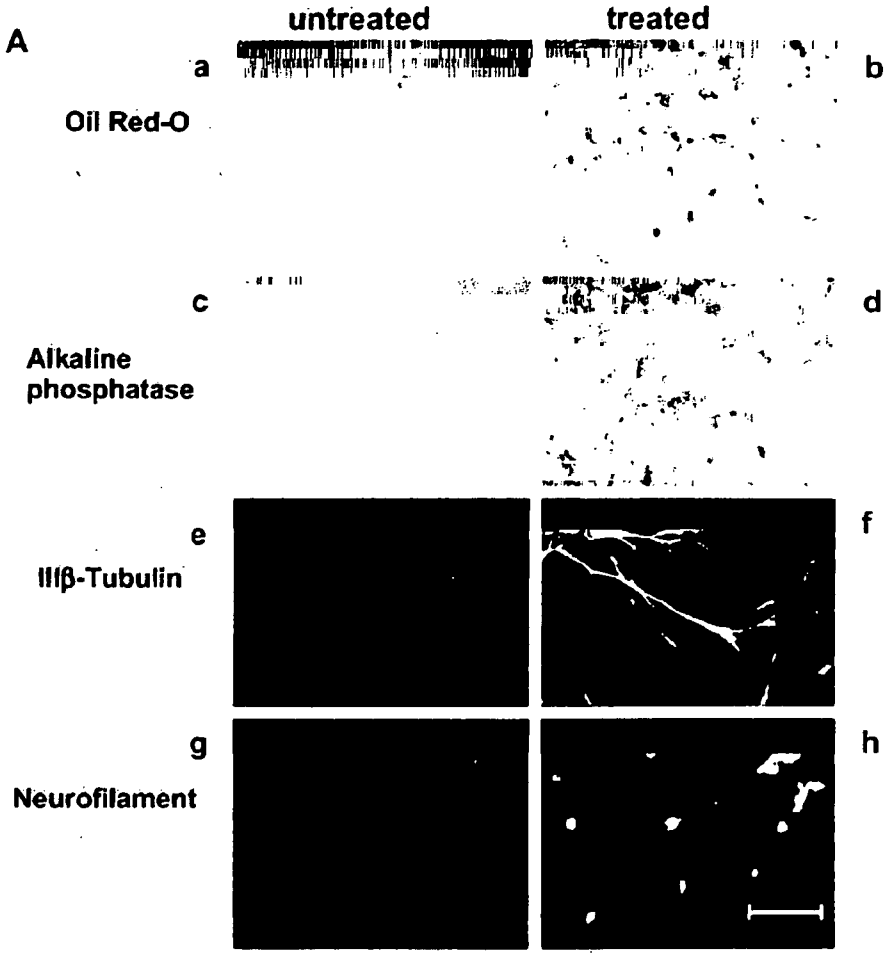

Figure 4. Differentiation potential of immortalized human mesenchymal stem cell lines into adipogenic, osteogenic, and neurogenic lineages. Adipogenesis was indicated by the accumulation of lipid stained with Oil Red-O (*Aa* and *Ab*, UE6E7T-3 cell line). Osteogenesis is indicated by the increase in alkaline phosphatase (*Ac* and *Ad*, UCB408E6E7TERT-33 cell line). Neurogenesis was shown by staining with two kinds of monoclonal antibodies to IIIβ-tubulin and neurofilament, and by shape changes of cell (*Ae–Ah*, UBE6T-6 cell line). *B*, Comparison of the differentiation potential of four cell lines whose responses to stimuli into differentiation were diverse among the cell lines. − and + indicate a response similar to an untreated cell and a weak positive response. +++ indicates a strong response shown by images of treated cells in Fig. 4*A*. (*Bar* indicates 20 μm).

B

	UCBTERT-21	UCB408E6E7TERT-33	UE6E7T-3	UBE6T-6
Oil Red-O	+	++	+++	+
Alkarine phosphatase	+	+++	+	+
IIIβ- Tubulin	-	+	+/-	+++
Neurofilament	-	++	-	++

whereas such changes were not evident with the flat-shaped cells before induction (Fig. 4*Ae*, *Ag*). Additionally, such cells did not undergo such differentiation in culture medium when cultured for as long as 30 d, although faint staining was observed. Figure 4*B* shows the overall results of differentiation potential of the four cell lines into adipogenic, osteogenic, and neurogenic lineages. These immortalized mesenchymal stem cell lines retained the ability to differentiate into three lineages, although among cell lines there are significant variations in response to lineage-specific induction.

Discussion

Attempts to clarify the mechanisms for extending the lifespan of tumor cells have been made for many years, and several genes that have effects on cellular proliferation and survival have become clear (Munger et al. 2002) in addition to the elucidation that the majority of tumor cells express telomerase (hTERT; Armanios et al. 2005). The goal of one of the series of our studies has been to establish cell lines with long lifespan and with parental properties, on the basis of genotypic and phenotypic characterizations, for application to cell-based therapy. We previously established several cell lines (Takeda et al. 2004; Mori et al. 2005; Terai et al. 2005), and the present study demonstrated that UCBTERT-21, the immortalized cell line derived from human umbilical cord blood-derived MSCs with hTERT, has a normal karyotype and has an extended lifespan by at least 133 population doublings, and has the differentiation potential into the adipocyte or osteoblast similar to parental MSCs (Terai et al. 2005), although the potential was weak but clearly positive in this study. The specific environmental cues to initiate the differentiation of hMSCs are not yet clear.

UCBTERT-21 immortalized with hTERT alone can be prolonged without inhibition of the $p16^{INK4A}$/RB pathway (Terai et al. 2005), the result of which is in agreement with reports that hTERT alone significantly extends the lifespan of human fibroblasts, epithelial, and endothelial cells (Bodnar et al. 1998; Chang et al. 2005), without the requirement for molecular alterations in p53/p21 and pRB/$p16^{INK4A}$ pathways (Milyavsky et al. 2003). However, other researchers have indicated that inactivation of the RB/p16 pathway by E7, or downregulation of p16 expression, in addition to increasing telomerase activities, is necessary for expanding the lifespan of human keratinocytes (Dickson et al. 2000; Kiyono et al. 1998). Thus, the possibility that a telomere-independent barrier may operate to prevent immortalization according to cell types has been indicated.

UCB408E6E7TERT-33, UE6E7T-3, and UBE6T-6 are hMSC-clones immortalized with HPV16E6/E7 or polycomb group oncogene Bmi-1, in combination with hTERT. Immortalization of human keratinocyte in vitro using virus-derived oncogenes such as E6 and E7 is based on initial inactivation of the p53 and/or Rb pathways, which are essential for controlling cell cycle progression in response to DNA damage or after induction tetraploidy; therefore, this gene transduction induces chromosomal abnormalities (Solinas-Toldo et al. 1997; Duensing et al. 2002; Patel et al. 2004; Schaeffer et al. 2004). The cell lines used in this study became completely immortal, yet underwent dynamic changes in their chromosome numbers in prolonged culture. Near diploid population in early passage of UCB408E6E7 TERT-33 became near-tetraploid population with prolonged culture without the appearance of intermediate populations (60–70 chromosomes/cell), and thereafter gave rise to a population having smaller numbers of chromosomes than tetraploid. Similar patterns existed, although at a slower rate, in UBE6T-6 cells and UE6E7T-3. These results suggest that HPVE6 and E7 proteins cause tetraploidy that precedes the chromosomal aberration to aneuploid in E6/E7-immotalized hMSCs, as is currently shown in several lines of evidence. For example, in vitro experiments in human cell lines (N/TERT-1 keratinocytes and HeLa cells) demonstrate that chromosome nondisjunction yields tetraploid rather than aneuploid, and that aneuploid may develop through chromosomal loss from tetraploid, although the mechanistic basis for the tetraploid formation still remains to be elucidated (Shi et al. 2005). This is also suggested from evidence that high frequency of tetraproidy is present with aneuploidy in human tumors (Olaharski et al. 2006; Sen 2000). A distinct pattern of aneuploid became apparent using dual-probe FISH and CGH analyses, in which UCB408E6E7TERT-33 cells predominantly exhibited triploid 13 and tetraploidy 17 together with other chromosomal changes as shown in Figs. 2 and 3. However, surprisingly, the loss of one copy of chromosome 13 was also seen in 70–80% of diploid UE6E7T-3 and diploid UBE6T-6 cells retaining two copies of chromosome 17. The loss occurred in PDL 50 in both UE6E7T-6 and UCB408E6E7TERT-33, and between PDL 78 and 101 in UE6E7T-3. Structural and numerical aberrations targeting chromosome 17 are often reported in tumors from various tissues (Olaharski et al. 2006), whereas the pattern that chromosome 13 is lost and chromosome 17 is stable, was common for the three cell lines in this study, indicating the possibility that the loss of chromosome 13 may play an important role in the chromosomal aberration of hMSC's to acquire growth advantages under the given culturing condition. Similar karyotypic changes were evident in cultured human embryonic stem cells, involving the gain of chromosome 17 or chromosome 12 (Carlson et al. 2000; Draper et al. 2004). It is thus conjectured that the aneuploidy developed through chromosomal loss from

diploid cells arises through different mechanisms from tetraploid intermediate.

An alternative explanation for aneuploid formation mechanism independent of tetraploid intermediate is loss of regulation in centrosome duplication, leading to abnormal centrosome amplification and multipolar spindles, resulting in aneuploidy. In addition, centrosome amplification caused by loss of p53 has been shown in cultured mouse cells (Fukasawa et al. 1996), but not in cultured human cells (Kawamura et al. 2004). However, loss of p53 and centrosome amplification has been revealed in human cancer tissue. Our preliminary examination has indicated a weak correlation between centrosome amplification and chromosome number (data not shown). Only 2.4% of UCBTERT-21 cells contained >3 centrosomes per cell, whereas 11.9% of UCB408E6E7TERT-33, 19.1% of UE6E7T-3 and 14.3% of UBE6T-6 cells contained >3 centrosomes per cell. Thus, further study is still needed to clarify the mechanism inducing chromosomal instability in immortalized hMSCs cultured over a long period.

Human mesenchymal stem cells are thought to be multipotent cells that can replicate stem cells and that can differentiate to lineages of mesenchymal tissues including bone, fat, tendon, and muscle. Our results indicated that immortalized hMSCs, except UCBTERT-21, induced changes in chromosome number over prolonged culture, but these cells have still retained the ability to both proliferate and differentiate. Immortalized UBE6T-6 cells also displayed neuron-like morphology and strong expression of the neuron-specific markers of neurofilament and III-β-tubulin. We previously demonstrated that hTERT, E7-immortalized hMSCs differentiate into neural cells in vitro on the basis of morphological changes, expression of neural markers such as nestin, neurofilament, MAP-2, Nurr1, and III-β-tubulin. Furthermore, the physiological function showed reversible calcium uptake in response to extracellular potassium concentration (Mori et al. 2005). Similar observations have been reported using rat MSCs (Wislet-Gendebien et al. 2003; Wislet-Gendebien et al. 2005; Pacary et al. 2006). In preliminary experiment of cell transplantation that 10^6 cells of UCBTERT-21 cell (PDLs 120) or UCB408E6E7TERT-33 cell (PDLs 200) were injected into nude mice subcutaneously, no tumorigenicity was observed (data not shown).

In conclusion, our study showed that the hTERT-immortalized cell line displayed normal karyotype and differentiation ability in prolonged culture. These results provide a step forward toward supplying a sufficient number of cells for new therapeutic approaches. In addition, oncogene-immortalized cell lines exhibited abnormal karyotype accompanying the preferential loss of chromosome 13 but without differential alteration during prolonged culture. Thus, the results could provide a useful model for understanding the mechanisms of the chromosomal instability and the differentiation of hMSC.

Acknowledgments This study was supported in part by a grant from the Ministry of Health, Labor and Welfare of Japan. We are grateful to Dr. T.Masui for his advice on ethics problems, and to Mr. H.Migitaka (Carl Zeiss Co., Ltd.) for his assistance with mFISH karyotype analysis. M.T. and K.T. contributed equally to this work.

References

Armanios, M.; Greider, C. W. Telomerase and cancer stem cells Cold Spring Harbor Symp. Quant. Biol. 70:205–208; 2005.

Bodnar, A. G.; Ouellette, M.; Frolkis, M.; Holt, S. E.; Chiu, C. P.; Morin, G. B.; Harley, C. B.; Shay, J. W.; Lichtsteiner, S.; Wright, W. E. Extension of life-span by introduction of telomerase into normal human cells. Science 279:349–352; 1998.

Burns, J. S.; Abdallah, B. M.; Guldberg, P.; Rygaard, J.; Schroder, H. D.; Kassem, M. Tumorigenic heterogeneity in cancer stem cells evolved from long-term cultures of telomerase-immortalized human mesenchymal stem cells. Cancer Res. 65:3126–3135; 2005.

Carlson, J. A.; Healy, K.; Tran, T. A.; Malfetano, J.; Wilson, V. L.; Rohwedder, A.; Ross, J. S. Chromosome 17 aneusomy detected by fluorescence in situ hybridization in vulvar squamous cell carcinomas and synchronous vulvar skin. Am. J. Pathol. 157:973 983; 2000.

Chang, M. W.; Grillari, J.; Mayrhofer, C.; Fortschegger, K.; Allmaier, G.; Marzban, G.; Katinger, H.; Voglauer, R. Comparison of early passage, senescent and hTERT immortalized endothelial cells. Exp. Cell Res. 309:121–136; 2005.

Cross, S. M.; Sanchez, C. A.; Morgan, C. A.; Schimke, M. K.; Ramel, S.; Idzerda, R. L.; Raskind, W. H.; Reid, B. J. A p53-dependent mouse spindle checkpoint. Science 267:1353–1356; 1995.

Dickson, M. A.; Hahn, W. C.; Ino, Y.; Ronfard, V.; Wu, J. Y.; Weinberg, R. A.; Louis, D. N.; Li, F. P.; Rheinwald, J. G. Human keratinocytes that express hTERT and also bypass a p16(INK4a)-enforced mechanism that limits life span become immortal yet retain normal growth and differentiation characteristics. Mol. Cell Biol. 20:1436–1447; 2000.

Draper, J. S.; Smith, K.; Gokhale, P.; Moore, H. D.; Maltby, E.; Johnson, J.; Meisner, L.; Zwaka, T. P.; Thomson, J. A.; Andrews, P. W. Recurrent gain of chromosomes 17q and 12 in cultured human embryonic stem cells. Nat. Biotechnol. 22:53–54; 2004.

Duensing, S.; Lee, L. Y.; Duensing, A.; Basile, J.; Piboonniyom, S.; Gonzalez, S.; Crum, C. P.; Munger, K. The human papillomavirus type 16 E6 and E7 oncoproteins cooperate to induce mitotic defects and genomic instability by uncoupling centrosome duplication from the cell division cycle. Proc. Natl. Acad.Sci. U. S. A. 97:10002–10007; 2000.

Duensing, S.; Munger, K. The human papillomavirus type 16 E6 and E7 oncoproteins independently induce numerical and structural chromosome instability. Cancer Res. 62:7075–7082; 2002.

Fukasawa, K.; Choi, T.; Kuriyama, R.; Rulong, S.; Vande Woude, G. F. Abnormal centrosome amplification in the absence of p53. Science 271:1744–1747; 1996.

Harada, H.; Nakagawa, H.; Oyama, K.; Takaoka, M.; Andl, C. D.; Jacobmeier, B.; von, W. A.; Enders, G. H.; Opitz, O. G.; Rustgi, A. K. Telomerase induces immortalization of human esophageal keratinocytes without p16INK4a inactivation. Mol. Cancer Res. 1:729–738; 2003.

Kawamura, K.; Izumi, H.; Ma, Z.; Ikeda, R.; Moriyama, M.; Tanaka, T.; Nojima, T.; Levin, L. S.; Fujikawa-Yamamoto, K.; Suzuki, K.; Fukasawa, K. Induction of centrosome amplification and

chromosome instability in human bladder cancer cells by p53 mutation and cyclin E overexpression. Cancer Res. 64:4800–4809; 2004.

Khan, S. H.; Wahl, G. M. p53 and pRb prevent rereplication in response to microtubule inhibitors by mediating a reversible G1 arrest. Cancer Res. 58:396–401; 1998.

Kiyono, T.; Foster, S. A.; Koop, J. I.; McDougall, J. K.; Galloway, D. A.; Klingelhutz, A. J. Both Rb/p16INK4a inactivation and telomerase activity are required to immortalize human epithelial cells. Nature 396:84–88; 1998.

Makino, S.; Fukuda, K.; Miyoshi, S.; Konishi, F.; Kodama, H.; Pan, J.; Sano, M.; Takahashi, T.; Hori, S.; Abe, H.; Hata, J.; Umezawa, A.; Ogawa, S. Cardiomyocytes can be generated from marrow stromal cells in vitro. J. Clin. Invest. 103:697–705; 1999.

Milyavsky, M.; Shats, I.; Erez, N.; Tang, X.; Senderovich, S.; Meerson, A.; Tabach, Y.; Goldfinger, N.; Ginsberg, D.; Harris, C. C.; Rotter, V. Prolonged culture of telomerase-immortalized human fibroblasts leads to a premalignant phenotype. Cancer Res. 63:7147–7157; 2003.

Mori, T.; Kiyono, T.; Imabayashi, H.; Takeda, Y.; Tsuchiya, K.; Miyoshi, S.; Makino, H.; Matsumoto, K.; Saito, H.; Ogawa, S.; Sakamoto, M.; Hata, J.; Umezawa, A. Combination of hTERT and bmi-1, E6, or E7 induces prolongation of the life span of bone marrow stromal cells from an elderly donor without affecting their neurogenic potential. Mol. Cell Biol. 25:5183–5195; 2005.

Munger, K.; Baldwin, A.; Edwards, K. M.; Hayakawa, H.; Nguyen, C. L.; Owens, M.; Grace, M.; Huh, K. Mechanisms of human papillomavirus-induced oncogenesis. J. Virol. 78:11451–11460; 2004.

Munger, K.; Howley, P. M. Human papillomavirus immortalization and transformation functions. Virus Res. 89:213–228; 2002.

Okamoto, T.; Aoyama, T.; Nakayama, T.; Nakamata, T.; Hosaka, T.; Nishijo, K.; Nakamura, T.; Kiyono, T.; Toguchida, J. Clonal heterogeneity in differentiation potential of immortalized human mesenchymal stem cells3. Biochem. Biophys. Res. Commun. 295:354–361; 2002.

Olaharski, A. J.; Sotelo, R.; Solorza-Luna, G.; Gonsebatt, M. E.; Guzman, P.; Mohar, A.; Eastmond, D. A. Tetraploidy and chromosomal instability are early events during cervical carcinogenesis. Carcinogenesis 27:337–343; 2006.

Pacary, E.; Legros, H.; Valable, S.; Duchatelle, P.; Lecocq, M.; Petit, E.; Nicole, O.; Bernaudin, M. Synergistic effects of CoCl(2) and ROCK inhibition on mesenchymal stem cell differentiation into neuron-like cells. J. Cell Sci. 119:2667–2678; 2006.

Patel, D.; Incassati, A.; Wang, N.; McCance, D. J. Human papillomavirus type 16 E6 and E7 cause polyploidy in human keratinocytes and up-regulation of G2-M-phase proteins. Cancer Res. 64:1299–1306; 2004.

Pittenger, M. F.; Mackay, A. M.; Beck, S. C.; Jaiswal, R. K.; Douglas, R.; Mosca, J. D.; Moorman, M. A.; Simonetti, D. W.; Craig, S.; Marshak, D. R. Multilineage potential of adult human mesenchymal stem cells. Science 284:143–147; 1999.

Saito, M.; Handa, K.; Kiyono, T.; Hattori, S.; Yokoi, T.; Tsuhakimoto, T.; Harada, H.; Noguchi, T.; Toyoda, M.; Sato, S.; Teranaka, T. Immortalization of cementoblast progenitor cells with Bmi-1 and TERT. J. Bone Miner. Res. 20:50–57; 2005.

Schaeffer, A. J.; Nguyen, M.; Liem, A.; Lee, D.; Montagna, C.; Lambert, P. F.; Ried, T.; Difilippantonio, M. J. E6 and E7 oncoproteins induce distinct patterns of chromosomal aneuploidy in skin tumors from transgenic mice. Cancer Res. 64:538–546; 2004.

Sen, S. Aneuploidy and cancer. Curr. Opin. Oncol. 12:82–88; 2000.

Shi, Q.; King, R. W. Chromosome nondisjunction yields tetraploid rather than aneuploid cells in human cell lines. Nature 437:1038–1042; 2005.

Solinas-Toldo, S.; Durst, M.; Lichter, P. Specific chromosomal imbalances in human papillomavirus-transfected cells during progression toward immortality. Proc. Natl. Acad. Sci. U. S. A. 94:3854–3859; 1997.

Takeda, Y.; Mori, T.; Imabayashi, H.; Kiyono, T.; Gojo, S.; Miyoshi, S.; Hida, N.; Ita, M.; Segawa, K.; Ogawa, S.; Sakamoto, M.; Nakamura, S.; Umezawa, A. Can the life span of human marrow stromal cells be prolonged by bmi-1, E6, E7, and/or telomerase without affecting cardiomyogenic differentiation? J. Gene Med. 6:833–845; 2004.

Takeuchi, K.; Kuroda, K.; Ishigami, M.; Nakamura, T. Actin cytoskeleton of resting bovine platelets. Exp. Cell Res. 186:374–380; 1990.

Terai, M.; Uyama, T.; Sugiki, T.; Li, X. K.; Umezawa, A.; Kiyono, T. Immortalization of human fetal cells: the life span of umbilical cord blood-derived cells can be prolonged without manipulating p16INK4a/RB braking pathway. Mol. Biol. Cell 16:1491–1499; 2005.

Wislet-Gendebien, S.; Hans, G.; Leprince, P.; Rigo, J. M.; Moonen, G.; Rogister, B. Plasticity of cultured mesenchymal stem cells: switch from nestin-positive to excitable neuron-like phenotype. Stem Cells 23:392–402; 2005.

Wislet-Gendebien, S.; Leprince, P.; Moonen, G.; Rogister, B. Regulation of neural markers nestin and GFAP expression by cultivated bone marrow stromal cells. J. Cell Sci. 116:3295–3302; 2003.

Zheng, L.; Lee, W. H. The retinoblastoma gene: a prototypic and multifunctional tumor suppressor. Exp. Cell Res. 264:2–18; 2001

In Vitro Cell.Dev.Biol.—Animal (2007) 43:168–175
DOI 10.1007/s11626-007-9033-5

Species identification of animal cells by nested PCR targeted to mitochondrial DNA

Kazumi Ono · Motonobu Satoh · Touho Yoshida · Yutaka Ozawa · Arihiro Kohara · Masao Takeuchi · Hiroshi Mizusawa · Hidekazu Sawada

Received: 5 March 2007 / Accepted: 17 April 2007 / Published online: 22 May 2007 / Editor: J. Denry Sato

Abstract We developed a highly sensitive and convenient method of nested polymerase chain reaction (PCR) targeted to mitochondrial deoxyribonucleic acid (DNA) to identify animal species quickly in cultured cells. Fourteen vertebrate species, including human, cynomolgus monkey, African green monkey, mouse, rat, Syrian hamster, Chinese hamster, guinea pig, rabbit, dog, cat, cow, pig, and chicken, could be distinguished from each other by nested PCR. The first PCR amplifies mitochondrial DNA fragments with a universal primer pair complementary to the conserved regions of 14 species, and the second PCR amplifies the DNA fragments with species-specific primer pairs from the first products. The species-specific primer pairs were designed to easily distinguish 14 species from each other under standard agarose gel electrophoresis. We further developed the multiplex PCR using a mixture of seven species-specific primer pairs for two groups of animals. One was comprised of human, mouse, rat, cat, pig, cow, and rabbit, and the other was comprised of African green monkey, cynomolgus monkey, Syrian hamster, Chinese hamster, guinea pig, dog, and chicken. The sensitivity of the PCR assay was at least 100 pg DNA/reaction, which was sufficient for the detection of each species of DNA. Furthermore, the nested PCR method was able to identify the species in the interspecies mixture of DNA. Thus, the method developed in this study will provide a useful tool for the authentication of animal species.

Keywords Cell line authentication · Cross-contamination · Quality control · Bio-resources

K. Ono · M. Satoh (✉) · T. Yoshida · H. Sawada
Health Science Research Resources Bank (HSRRB),
Japan Health Sciences Foundation,
2-11-Rinku-minamihama, Sennan-shi,
Osaka 590-0535, Japan
e-mail: hsrrb@osa.jhsf.or.jp

Y. Ozawa · A. Kohara · M. Takeuchi · H. Mizusawa
Japanese Collection of Research Bioresources (JCRB),
Division of Bioresources,
National Institute of Biomedical Innovation,
7-6-8 Saito-Asagi, Ibaraki-shi,
Osaka 567-0085, Japan

Introduction

It has been occasionally reported that cell lines derived from a certain source can be contaminated with another cell line. This cross-culture contamination is a serious problem for investigations using culture cells (Nelson-Rees et al. 1981). Therefore, it is very important to confirm the identities of cell lines as part of quality control in the operation of the cell banks that supply these cells to researchers. Some methods have been developed for the authentication of cell lines. For example, short tandem repeat profiling has been used to identify human-origin cell lines (Tanabe et al. 1999; Masters et al. 2001). As for the methods to detect interspecies cross-contamination, chromosome typing, immunological testing, and isoenzyme analysis have been used (Montes de Oca et al. 1969; Stulberg 1973; Doyle et al. 1990). Each of these methods, however, has disadvantages, such as chromosome analysis, which requires great skill, and immunological identification, which requires species-specific antibodies. Isoenzyme analysis is a general method to find

interspecies cross-contamination (Steube et al. 1995). However, the sensitivity of this technique is not suitable for the detection of intermingling with other species-derived cells (Nims et al. 1998), and some specialized reagents and devices are required.

The identification of species by polymerase chain reaction (PCR) based on species-specific deoxyribonucleic acid (DNA) sequences has many advantages, as follows: (1) the equipment required for PCR has become widespread in the laboratories of life science research, (2) the method is relatively simple and does not require great skill, and (3) the sensitivity is high because of amplification of a specific DNA fragment. Thus, some PCR methods for identification of animal species, including cell line authentication, have been reported in recent years (Naito et al. 1992; Hershfield et al. 1994; Parodi et al. 2002; Liu et al. 2003; Steube et al. 2003). However, these methods are not suitable for the purpose of rapidly distinguishing many kinds of animal species.

In the present study, we developed a highly sensitive PCR method that can distinguish 14 animal species, which are commonly used in cell cultures for life science research; i.e., human, cynomolgus monkey, African green monkey, mouse, rat, Syrian hamster, Chinese hamster, guinea pig, rabbit, dog, cat, cow, pig, and chicken.

Materials and Methods

Cell lines and preparation of DNA. All cell lines used in this study are shown in Table 1 and are available from the Health Science Research Resources Bank (HSRRB). These cell lines were confirmed to be free of microorganisms, such as mycoplasma, bacteria, fungi and yeast, and the species in the original description was authenticated by isoenzyme analysis at the HSRRB. Cellular DNA containing both nuclear and mitochondrial DNA was extracted using MagExtractor-Genome (Toyobo. Co., Ltd., Osaka, Japan) according to the manufacturer's instruction, and the resultant purified DNA was used for PCR.

Primer design. The information of full-length and partial mitochondrial DNA sequences for 14 species of animals were obtained from the published database at the National Center for Biotechnology Information (NCBI). The accession numbers of the reference sequences and the area corresponding to each primer's target are listed in Table 2, and the nucleotide sequences of each primer are presented in Table 3. The first primers, which were complementary to conserved sequences within cytochrome *b* (for forward primer) and 16S ribosomal RNA genes (for reverse) among the 14 species, were designed as a universal primer pair (Fig. 1). The amplified product covers cytochrome *b*, d-loop, 12S ribosomal RNA and 16S ribosomal RNA genes, and the predicted product size is 4–5 kbp. The species-specific sequences within the area amplified by the universal primer pair were selected as second primer pairs. To clearly identify the species-specific bands in agarose gel electrophoresis, we designed 2nd primers for the 14 species to amplify different sizes of DNA in the range of 200–1400 bp at approximately 50-bp intervals (Table 2; see also Fig. 3*A*).

Polymerase chain reaction. The 50-μl reaction mixture contained 1.25 units Takara Ex Taq (Takara Bio, Inc., Otsu, Japan), Ex Taq buffer (Mg^{2+}: 2 mM), dNTPs (50 μM each), 10 pmol of each primer and 100 ng of sample DNA, unless otherwise stated. The amplification was carried out in a PCR Thermal Cycler MP (TP3000; Takara Bio Inc.). In the first PCR, the reaction mixture was heated at 94° C for 5 min, at 59° C for 5 min, followed by 35 cycles of elongation at 72° C for 2.5 min, denaturation at 94° C for 30 s, annealing at 59° C for 45 s, with elongation at 72° C

Table 1. Cell lines used in this study

Name of cell line	Registry number	Species
293	JCRB9068	Human
A549	JCRB0076	Human
COLO320 DM	JCRB0225	Human
HuH-7	JCRB0403	Human
HeLa S3	JCRB9010	Human
Hep G2	JCRB1054	Human
JTC-12	JCRB0607	Cynomolgus monkey
MK.P3	JCRB0607.1	Cynomolgus monkey
COS-7	JCRB9127	African green monkey
Vero	JCRB9013	African green monkey
3T3-L1	JCRB9014	Mouse
A9	JCRB0221	Mouse
B16 melanoma	JCRB0202	Mouse
KUM3	JCRB1134	Mouse
WEHI-3b	IFO50296	Mouse
C6	IFO50110	Rat
L6	JCRB9081	Rat
Py-3Y1-S2	JCRB0736	Rat
WB-F344	JCRB0193	Rat
BHK(C-13)	JCRB9020	Syrian hamster
RPMI 1846	JCRB9087	Syrian hamster
CHO-K1	IFO50414	Chinese hamster
TG-1	JCRB0626	Chinese hamster
104C1	JCRB9036	Guinea pig
SIRC	IFO50020	Rabbit
MDCK	IFO50071	Dog
CRFK	JCRB9035	Cat
PG4(S+L−)	JCRB9125	Cat
MDBK	JCRB9028	Cow
PK(15)	JCRB9030	Pig
DT40	JCRB9130	Chicken
LMH	JCRB0237	Chicken
4G12 hybridoma	IFO50090	Hybrid (human × mouse)
N18-RE-105	IFO50221	Hybrid (mouse × rat)

Table 2. The target sequence position for each primer pair in the mitochondrial genome and the predicted size of the amplified product

Species	Primer						Reference mitochondrial DNA sequence (NCBI accession number)
	First primer		Second primer				
	Forward	Reverse	Forward	Reverse	Genes amplified	Predicted product size (bp)	
Human	15226–15249	2990–3009	15311–15334	15732–15751	Cyt b	441	NC 001807
Cynomolgus monkey	479–502[(a)]	1572–1591[(b)]	209–229[(c)]	1320–1340[(c)]	12S→16S	1132	(a)AF295584, (b)AF420036, (c)AF424970
African green monkey	14643–14666	2408–2427	800–823	1074–1100	12S→16S	301	AY863426.1
Mouse	14623–14646	2430–2449	28–55	954–975	tRNA-Phe→12S	948	NC 005089
Rat	14602–14625	2419–2438	1748–1767	2218–2240	16S	493	NC 001665
Syrian hamster	479–502	ND[a]	682–703	906–926	Cyt b	245	AF119265
Chinese hamster	14604–14627	2413–2432	353–376	930–953	12S	601	DQ390542
Guinea pig	14642–14665	2494–2413	140–159	454–478	12S	339	NC 000884
Rabbit	14653–14676	2425–2444	116–136	799–819	12S	704	NC 001913
Dog	14668–14691	2428–2447	1105–1125	1838–1859	16S	755	AY729880
Cat	15516–15539	3288–3307	1675–1694	3046–3065	12S→16S	1391	NC 001700
Cow	14991–15014	2781–2800	401–421	1469–1490	tRNA-Phe→16S	1090	AB074965
Pig	15791–15814	3568–3587	2099–2123	2898–2917	12S→16S	819	AY337045
Chicken	15383–15406	3715–3734	3395–3415	3570–3591	16S	197	AB086102

Cyt b cytochrome b, *tRNA-Phe* phenylalanine transfer RNA, *12S* 12S ribosomal RNA, and *16S* 16S ribosomal RNA
[a] The corresponding 16S ribosomal RNA genome sequence of Syrian hamster was not available.
[(a)] means reference sequence AF295584.
[(b)] means reference sequence AF420036.
[(c)] means reference sequence AF424970.

for 10 min in the last cycle, and stored at 4° C. The first amplified product was diluted to 1:10 with sterile distilled water, and a 1 μl aliquot of the diluted product was used as the sample DNA for the second PCR. In the second PCR, the reaction mixture was heated to 94° C for 5 min, maintained at 60° C for 5 min, followed by 30 cycles of elongation at 72° C for 1.5 min, denaturation at 94° C for 45 s, annealing at 60° C for 30 s, with elongation at 72° C for 10 min in the last cycle, and stored at 4° C. Each 5 μl of second PCR product was run on a 2% agarose (SeaKem GTG agarose; Cambrex Bio Science Rockland, Inc., Rockland, ME) minigel unless otherwise noted, stained

Table 3. Nucleotide sequences of each primer pair

Primer pair	Forward sequence	Reverse sequence
First PCR primer	THGTHSAATGAATCTGAGGVGGVT	CGATGTTGGATCAGGACATC
Second PCR primer		
Human	TATTGCAGCCCTAGCAGCACTCCA	AGAATGAGGAGGTCTGCGGC
Cynomolgus monkey	AGTGAGCGCAAACGCCACTGC	GTTAACAGTGAAGGTGGCATG
African green monkey	CCAGAAGACCCACGATAACTCTCA	TGTTAGCTCAAGGTAATCGAGTTGTAC
Mouse	GCACTGAAAATGCTTAGATGGATAATTG	CCTCTCATAAACGGATGTCTAG
Rat	CAATCCACCAAGCACAAGTG	CCCCAACCGAAATTTGGTAGTTC
Syrian hamster	GACCTCTTAGGTGTATTCCTAC	GTATGAAGAAGGGGTAGAGCA
Chinese hamster	CCGGCGTAAAACGTGTTATAGACT	GTATTAGGTATAATATCGGCAGTC
Guinea pig	GCCCTATGTACCACACTCAG	CCTTAGCTTTCGTGTGTCGGACTTA
Rabbit	CATGCAAGACTCCTCACGCCA	GGGCTTTCGTATATTCTGAAG
Dog	GCCCAACTAACCCCAAACTTA	GGTTAACAATGGGGTGGATAAG
Cat	TAGAACACCCACGAAGATCC	CATATGGTCTCTTTGGGTCG
Cow	CCTAGATGAGTCTCCCAACTC	GTTGTTTAGTCGAGAGGGTATC
Pig	CCTATATTCAATTACACAACCATGC	GCGTGTGCGAGGAGAAAGGC
Chicken	GTATTCCCGTGCAAAAACGAG	CTTAGTGAAGAGTTGTGGTCTG

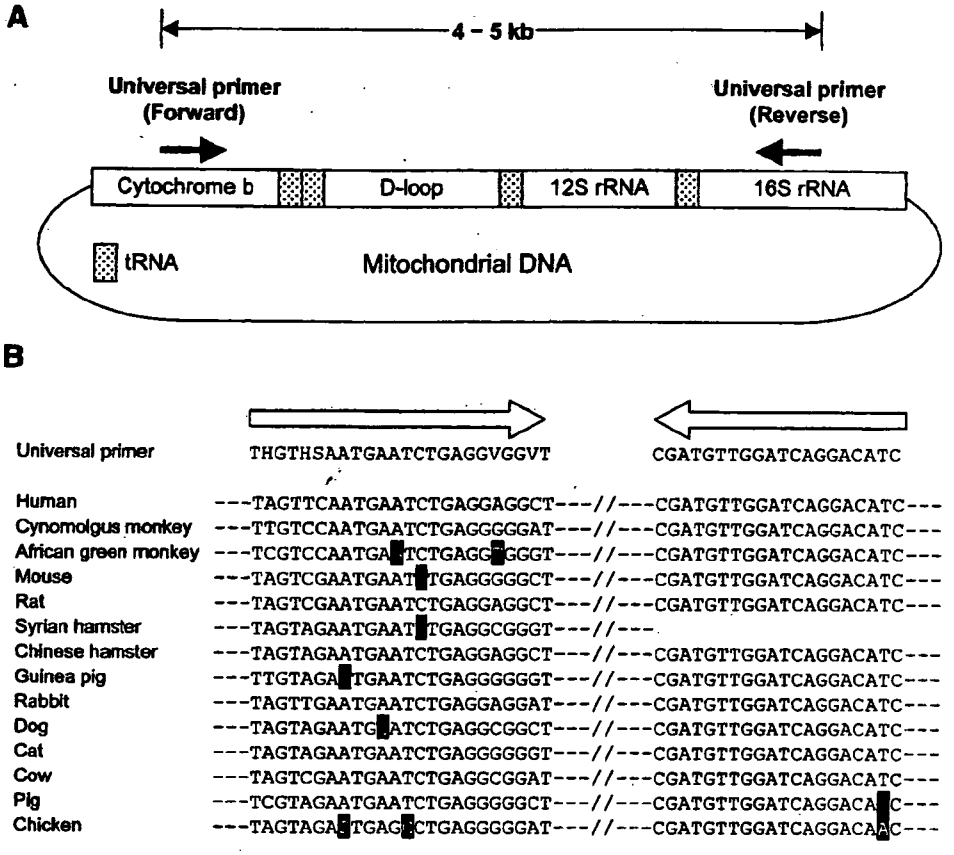

Figure 1. Universal primer pairs for the first PCR. (*A*) The target position in the mitochondrial DNA. The first PCR is expected to amplify 4- to 5-kb DNA fragments spanning from cytochrome *b* to 16S rRNA. (*B*) The sequences of the universal primers and the target nucleotide of 14 animal species. The forward primer was designed to be complementary to the conserved sequences within cytochrome *b* and the reverse primer within 16S ribosomal RNA, respectively. Degenerate primer was used for the forward primer, i.e., H;A/C/T, S;C/G, V;A/C/G. Inversed letters indicate bases mismatched to universal primer sequences. The 16S rRNA sequence of Syrian hamster for reverse primer was not available from the NCBI database.

with ethidium bromide, visualized under UV light (Mupid-Scope WD; Advance Co., Ltd., Tokyo, Japan), and photographed. The 100 bp DNA Ladder (Takara Bio Inc.) was applied as a size marker.

Result and Discussion

First PCR. Mitochondrial DNA is generally a desirable target for PCR compared with nuclear DNA, as each animal cell generally contains 500–1,000 copies of mitochondrial DNA. Primers were designed as described in "Materials and Methods". Figure 2 shows the gel electrophoresis of the first PCR products amplified with the universal primer pair from each species DNA. The predicted 4- to 5-kbp products were clearly observed for all species, except for chicken. In the case of chicken, no visible band was observed at ca. 5 kbp, the size predicted from chicken mitochondrial DNA sequence. However, it is likely that specific amplification does occur during the first PCR for chicken DNA, because a much larger amount of chicken DNA was required without first PCR for identification during the second PCR compared with that obtained when first PCR was carried out (data not shown).

Species-specificity of nested PCR. The nested PCR strategy was used to specifically amplify species-specific DNA. To confirm amplification by each species-specific primer pair, DNA prepared from each cell line originating from 14 species of animals was subjected to the nested PCR using the universal primer pair in the first PCR and the respective single species-specific primer pair in the second PCR. The amplified product from the corresponding species DNA exhibited the predicted size (Table 2) for each animal species, and could be readily distinguished from each other according to the different sizes (Fig. 3*A*). Figure 3*B* shows the species-specificity of nested PCR in this strategy. Most of the species-specific primer pairs, i.e., human, cynomolgus monkey, Syrian hamster, Chinese ham-

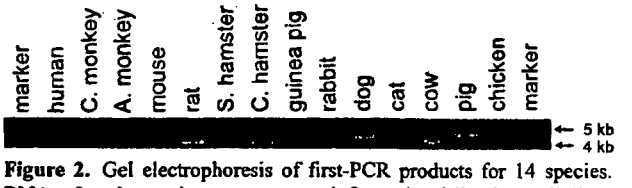

Figure 2. Gel electrophoresis of first-PCR products for 14 species. DNA of each species was extracted from the following cell lines indicated in *parentheses*, human (A549), cynomolgus monkey (MK. P3), African green monkey (COS-7), mouse (WEHI-3b), rat (Py-3Y1-S2), Syrian hamster (BHK-1 (C-13)), Chinese hamster (CHO-K1), guinea pig (104C1), rabbit (SIRC), dog (MDCK), cat (PG-4(S+L−)), cow (MDBK), pig (PK15), chicken (LMH) for amplification using the universal primer pair. The amplified DNA fragments were run on a 1% agarose gel.

ster, guinea pig, dog, cat, cow, pig, and chicken primers, amplified the specific DNA only from the corresponding species DNA. In the PCR using primer pairs specific for rabbit and African green monkey, however, unexpected bands appeared in addition to the predicted ones. The rabbit primer pair amplified cynomolgus monkey DNA, but the product could be readily distinguished from the rabbit-specific band because of their different sizes. The primer pair for African green monkey also produced an approximately 300-bp-sized band for cynomolgus monkey DNA, which was similar in size

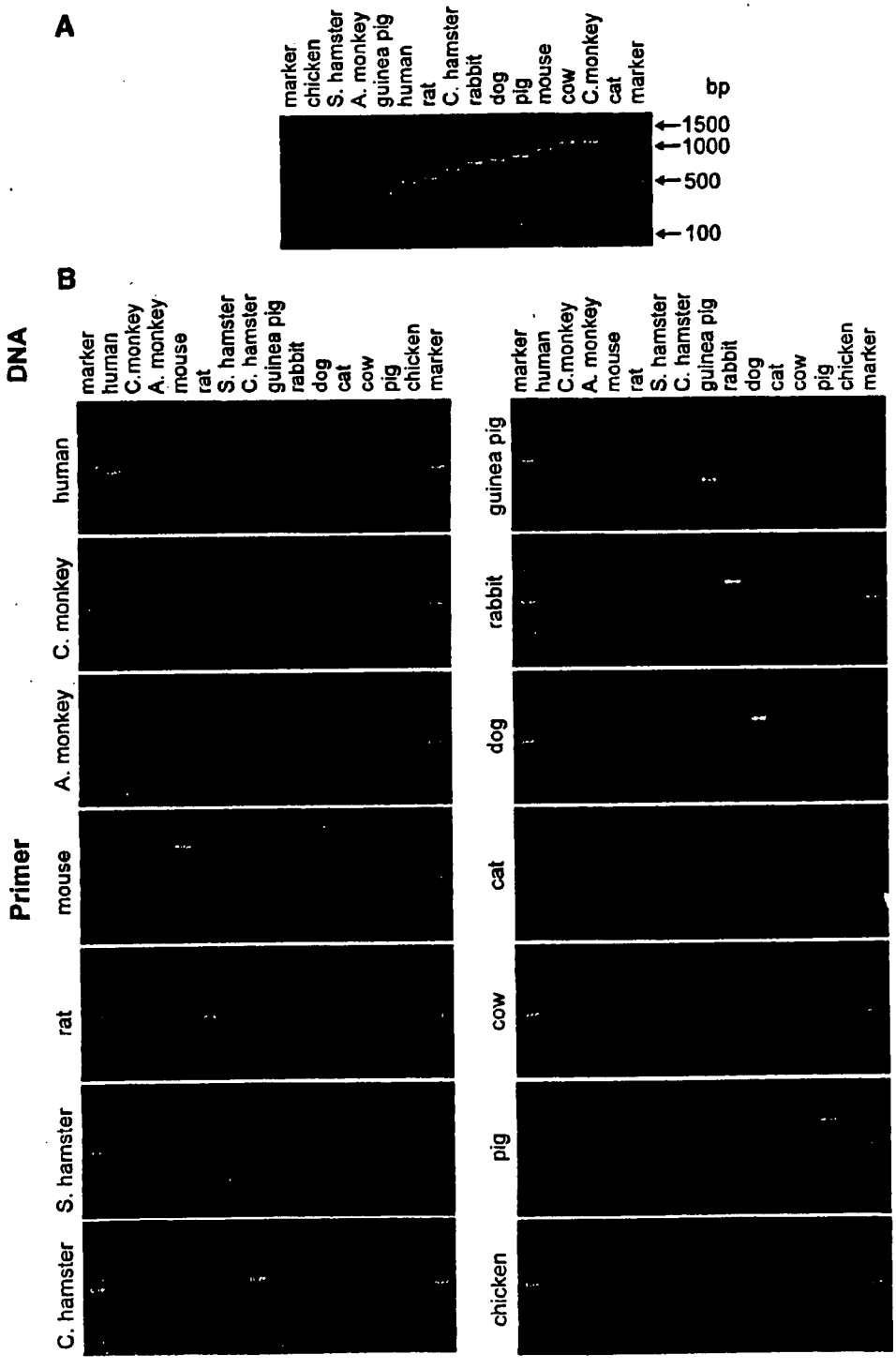

Figure 3. Gel electrophoresis of the second-PCR products for 14 species. The same cell lines as in Fig. 2 were used. (*A*) DNA of each species was subjected to nested PCR using corresponding species-specific primer pairs in the second PCR. The second-PCR products were aligned in size-order as a ladder. The amplification products were distinguished by the size. (*B*) Species specificity of the nested PCR. The 14 species-derived DNA was amplified with the universal primer pair and further amplified with the second primer pair indicated on the left side of each photograph.

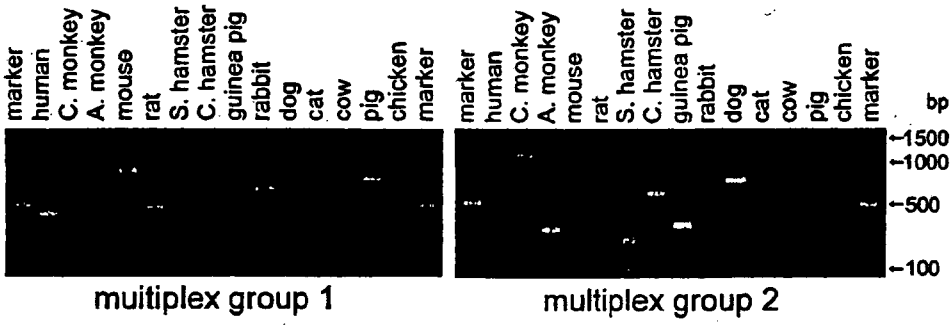

Figure 4. Gel electrophoresis of multiplex-PCR products. The first amplification products for 14 species DNA were subjected to multiplex PCR using the mixture of seven species-specific primer pairs as follows. Multiplex group 1: the primer mixture for human, mouse, rat, rabbit, cat, cow, and pig. Multiplex group 2: the primer mixture for cynomolgus monkey, African green monkey, Syrian hamster, Chinese hamster, guinea pig, dog, and chicken. The cell lines used for each animal are the same as described in Fig. 2.

to the African green monkey-specific product. This may be caused by some degree of sequence similarity between African green monkey and cynomolgus monkey in the target mitochondrial DNA. Indeed, when the mixture of primer pairs for African green monkey and cynomolgus monkey were applied to the second PCR, the nonspecific amplified product from cynomolgus monkey DNA disappeared, possibly because of competition of primer annealing to the target DNA sequences (data not shown; *see* also the result in the multiplex PCR section). Thus, it was confirmed that the nested PCR strategy is very useful for the identification of 14 species of DNA.

Multiplex PCR assay. For the simple and rapid identification of 14 species of animals, multiplex PCR was examined using primer mixtures in the second PCR. As a result of testing many combinations, it was favorable that the 14 kinds of species-specific primer pairs were divided into two groups as follows: Group 1 contained primer pairs for human, mouse, rat, rabbit, cat, cow, and pig, and Group 2 contained primers for cynomolgus monkey, African green monkey, Syrian hamster, Chinese hamster, guinea pig, dog, and chicken. Figure 4 shows the result of multiplex PCR. These animal species, divided into the two groups, could be clearly detected as species-specific bands. Most of the amplification products were specific for each primer mixture, but nonspecific bands were slightly observed for cynomolgus monkey and African green monkey when multiplex group 1 was used. These nonspecific bands were readily distinguished from the specific ones according to their sizes. Thus, it was found that multiplex PCR assay is applicable to simultaneous identification of 14 species of animals by dividing into two groups. The method developed here is superior to the previous PCR methods (Naito et al. 1992; Hershfield et al. 1994; Parodi et al. 2002; Liu et al. 2003; Steube et al. 2003) in identifying many kinds of species generally used for life science studies. In particular, this method has a great advantage in distinguishing Chinese hamster from Syrian hamster, as the cell lines such as CHO and BHK derived from these two kinds of hamsters are very popular for cell cultures.

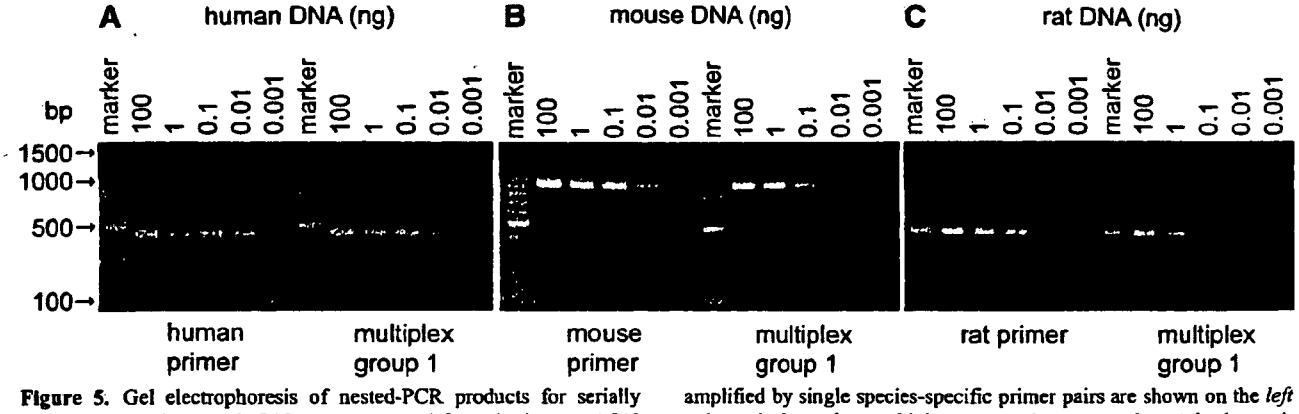

Figure 5. Gel electrophoresis of nested-PCR products for serially diluted DNA. The sample DNA was extracted from the human A549 cell line (*A*), mouse WEHI-3b cell line (*B*), and rat Py-3Y1-S2 cell line (*C*), and diluted serially to the nested PCR. The product bands amplified by single species-specific primer pairs are shown on the *left side* and those by multiplex group 1 are on the *right* in each photograph.

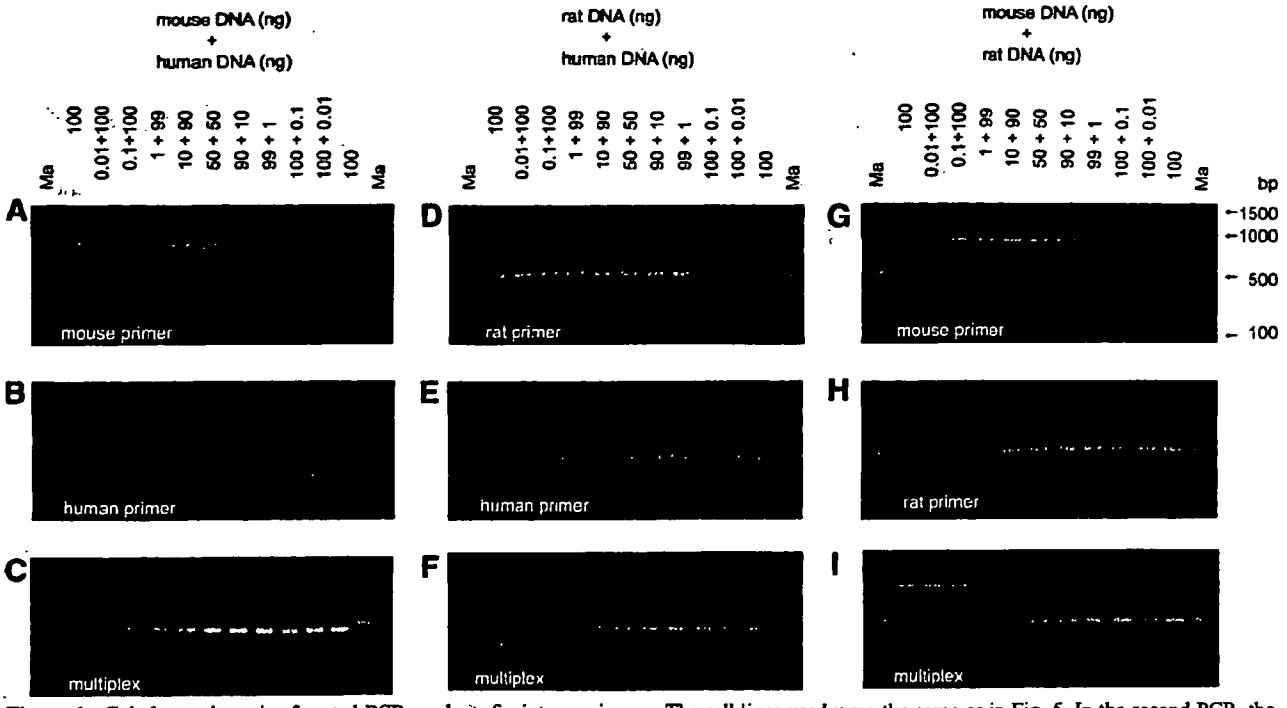

Figure 6. Gel electrophoresis of nested-PCR products for interspecies DNA mixtures. Two kinds of DNA, such as human and mouse DNA (*A, B, C*), human and rat DNA (*D, E, F*), and mouse and rat DNA (*G, H, I*) were mixed in various ratios for amplification with nested PCR. The cell lines used were the same as in Fig. 5. In the second PCR, the single species-specific primer pairs (*A, B, D, E, G, H*) or the multiplex group 1 (*C, F, I*) were used.

Sensitivity of PCR assay. Serially diluted cellular DNA was amplified with the nested PCR using either the corresponding species-specific primer pair or the mixture of seven species-specific primer pairs (multiplex PCR described above) as the second PCR primer. Each of the 14 species of DNA was detectable from at least 100 pg DNA/reaction by both PCR assays. Figure 5 shows the sensitivity of the PCR assay, as an example, using DNA prepared from human, mouse, and rat cell lines, which are commonly used for cell culture experiments. The amount of DNA required for identification of each species was 10 pg/reaction or more for the single species-specific primer pair as the second primer, and 100 pg/reaction or more for the multiplex assay. The sensitivity of the multiplex assay was somewhat low compared to the species-specific single primer.

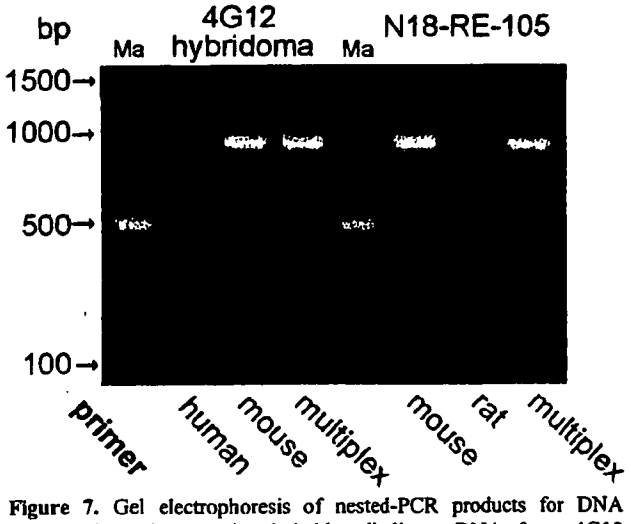

Figure 7. Gel electrophoresis of nested-PCR products for DNA derived from interspecies hybrid cell lines. DNA from 4G12 hybridoma (human × mouse) and N18-RE-105 (mouse × rat) were applied to nested PCR. Multiplex group 1 or the corresponding species-specific primer pairs were used in the second PCR.

Identification of species from interspecies DNA mixtures. The possibility of cross-contamination or replacement of cells exists during the process of cell preparation. As part of the quality control of cell lines in the cell bank, it is very important to verify the source species of each derived cell line. For that purpose, we attempted to identify the species from interspecies DNA mixtures. Two species of DNA, among human, mouse and rat, were mixed in various ratios for the nested PCR. When the single species-specific primer pair was used in the second PCR, each species of DNA was sensitively detected even when two kinds of DNA were present in the mixture. For example, when mouse-specific primers were used, a mouse-specific band was detected in the DNA mixture composed of 100 ng human or rat DNA + 10 pg mouse DNA (Fig. 6*A, G*). Likewise, in the case of human-specific or rat-specific primers alone, their respective species-specific band was also detected at 10 pg DNA

(Fig. 6*B, E, D, H*). When group 1 of the multiplex primers (seven species-specific primer pairs composed of human, mouse, rat, rabbit, cat, cow, and pig) was used at the standard concentration (10 pmol each species-specific primer/50-μl reaction), the sensitivity apparently decreased and there was considerable difference in the sensitivity for human, mouse, and rat DNA (Fig. 6*C, F, I*). This may be caused by the different amplification efficiency of each species-specific primer in the simultaneous reaction. Indeed, by decreasing the ratio of human primer pairs relative to the others, the sensitivity for mouse and rat DNA clearly increased (data not shown). Thus, this method will likely become a very useful tool for quickly detecting cross-contamination, and the sensitivity in the multiplex assay will be further increased by optimizing the concentration and the ratio of species-specific primers.

Hybrid cell lines. We applied this PCR method to original-species verification of interspecies hybrid cell lines. The hybrid cell lines of 4G12 (human B lymphocytes × mouse myeloma cell line; Saito et al. 1988) and N18-RE-105 (mouse glioma cell line × rat neural retina cells; Malouf et al. 1984) were tested by isoenzyme analysis and nested PCR. Although the original species were confirmed by isoenzyme analysis of both hybridomas between human and mouse, and between mouse and rat, only the mouse-specific band was observed for both hybridomas by nested PCR (Fig. 7). This result is consistent with the previous reports that the mouse mitochondria dominate selectively in these hybrid cells, whereas human or rat mitochondria are ultimately excluded from the hybrid cells (Attardi and Attardi 1972; Yamaoka et al. 2001). The nested PCR method targeted to the mitochondria genome was not applicable to the parental species identification of interspecies hybrid cells.

References

Attardi, B., Attardi, G. Fate of mitochondrial DNA in human-mouse somatic cell hybrids. Proc Nat Acad Sci USA. 129–133; 1972.

Doyle, A., Morris, C., Mowles, J. M. Quality control. In: Doyle, A, Hay, R., Kirsop, B. E. eds. Living resources for biotechnology. Animal cells. Chapter 5. Cambridge: Cambridge University Press; 1990: 81–100.

Hershfield, B., Chader, G., Aguirre, G. A polymerase chain reaction-based method for the identification of DNA samples from common vertebrate species. Electrophoresis. 15: 880–884; 1994.

Liu, M. Y., Lin, S., Liu H., Candal, F., Vafai A. Identification and authentication of animal cell culture by polymerase chain reaction amplification and DNA sequencing. In Vitro Cell Dev Biol Anim. 39: 424–427; 2003.

Malouf, A. T., Schnaar, R. L., Coyle, J. T. Characterization of a glutamic acid neurotransmitter binding site on neuroblastoma hybrid cells. J Biol Chem. 259: 12756–12762; 1984.

Masters, J. R., Thomson, J. A., Daly-Burns, B., Reid, Y. A., Dirks, W. G., Packer, P., Toji, L. H., Ohno, T., Tanabe, H., Arlett, C. F., Kelland, L. R., Harrison, M., Virmani, A., Ward, T. H., Ayres, K. L., Debenham, P. G. Short tandem repeat profiling provides an international reference standard for human cell lines. Proc Nat Acad Sci USA. 98: 8012–8017; 2001.

Montes de Oca, F., Macy, M. L., Shannon, J. E. Isoenzyme characterization of animal cell culture. Proc Soc Exp Biol Med. 132: 462–469; 1969.

Naito, E., Dewa, K., Yamanouchi, H., Kominami, R. Ribosomal ribonucleic acid (rRNA) gene typing for species identification. J Forensic Sci. 37: 396–403; 1992.

Nelson-Rees, W. A., Daniels, D. W., Flandermeyer, R. R. Cross-contamination of cells in culture. Science. 212: 446–452; 1981.

Nims, R. W. Shoemaker, A. P., Bauernschub, M. A., Rec L. J., Harbell, J. W. Sensitivity of isoenzyme analysis for the detection of interspecies cell line cross-contamination. In Vitro Cell Dev Biol Anim. 34: 35–39; 1998.

Parodi, B., Aresu, O., Bini, D., Lorenzini, R., Schena, F., Visconti, P., Cesaro, M., Ferrera, D., Andreotti, V., Ruzzon, T. Species identification and confirmation of human and animal cell lines: a PCR-based method. BioTechniques. 32: 432–440; 2002.

Saito, H., Uchiyama, K., Nakamura, I., Hiraoka, H., Yamaguchi, Y., Taniguchi, M. Characterization of a human monoclonal antibody with broad reactivity to malignant tumor cells. J Natl Cancer Inst. 80: 728–734; 1988.

Steube, K. G., Grunicke, D., Drexler, H. G. Isoenzyme analysis as a rapid method for the examination of the species identity of cell cultures. In Vitro Cell Dev Biol Anim. 31: 115–119; 1995.

Steube, K. G., Meyer, C., Uphoff, C. C., Drexler, H. G. A simple method using β-globin polymerase chain reaction for the species identification of animal cell lines—a progress report. In Vitro Cell Dev Biol Anim. 39: 468–475; 2003.

Stulberg, C. S. Extrinsic cell contamination of tissue culture. In: Fogh, J. ed. Contamination in tissue culture. New York: Academic Press; 1973:2–23.

Tanabe, H., Takada, Y., Minegishi, D., Kurematsu, M., Masui, T., Mizusawa, H. Cell line individualization by STR multiplex system in the cell bank found cross-contamination between ECV304 and EJ-1/T24. Tissue Culture Research Communications. 18: 329–338; 1999.

Yamaoka, M., Mikami, T., Ono, T., Nakada, K., Hayashi, J. Mice with only rat mtDNA are required as models of mitochondrial diseases. Biochem Biophys Res Commun. 282: 707–711; 2001.

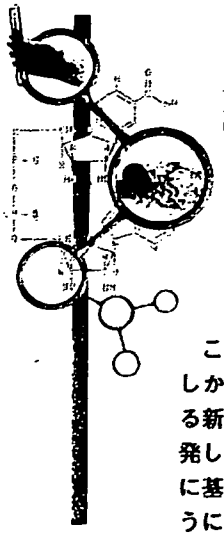

論理的分子設計に基づく創薬

水谷実穂，板井昭子

この10年，国内外の製薬企業ではできるだけ多くの化合物を保有し合成しアッセイすることに専念してきた．しかし，期待された程の成果は得られていない．生命や生体メカニズムの解明が進んでいるにも拘らず，開発される新薬は年々益々少なくなっている．筆者らは長い間，分子の三次元構造に基づく論理的医薬分子設計の方法を開発してきたが，近年はその方法を利用して自社テーマで創薬を行っている．その結果，標的タンパク質の構造情報に基づく計算シミュレーションに合成とアッセイを組合わせることで成功率高く効率よく医薬候補を開発できるようになっている．本稿ではその基本的な考え方について述べる．

はじめに

近年，ライフサイエンスの進歩は目覚しく，生体や生命の仕組みの解明と共に，疾患の分子メカニズムの解明が急速に進んでいる．新たな創薬標的の発見は創薬パラダイムに大きな変化をもたらした．かつて創薬は標的やメカニズムが不明のまま有機合成化学中心に既存薬や生体内物質に基づいて行われてきたが，近年は創薬のスタート時に標的タンパク質を設定するのが普通である．しかし，どんなに生体の仕組みの解明が進み，有望な標的が明らかになっても，薬を創製する難しさは変わらず，上市される新薬の数は減る一方である．

タンパク質分子や抗体を医薬とする高分子医薬は別として，低分子医薬の開発には出発点とする活性化合物の構造（医薬シードまたはリードと呼ぶ）に基づいて，設計・合成・評価を繰返して最適な化合物を探索する（リード最適化）過程が必須である．医薬シードの発見・創製は有効な方法がないために長い間不可能とされてきたが，1995年頃から，市販化合物・社内化合物からなる数十万ー数百万化合物のライブラリを片端からスクリーニングするHTS（高効率に自動的にランダムスクリーニング）システムにより，標的への結合活性や阻害活性をみることで可能になった．こうして見つけた弱い *in vitro* 活性化合物を合成展開して，最適な活性・動態をもち低毒性の化合物に導くことで創薬が目指されたが，期待したほどうまくいっていない．

近年はHTSだけでなく，多種の化合物の同時自動合成を目指すコンビナトリアル合成も含め，できるだけ多くの化合物を保有し，測るものが勝つという力づく信仰に陰りが見えており，創薬の成功率の向上・効率化・迅速化を可能にする論理的なアプローチへの関心が高まっている．

分子の三次元構造

リード最適化を論理的に進める方法として，40年程前から置換基の性質や大きさと活性の相関を統計的に探る定量的構造活性相関法（QSAR）があるが，母核が同じ誘導体系列でしか成立せず，多数の誘導体の合成後でしか使えないなど，後付けで論文作成用の便利なツールの域を出なかった．1980年以降，タンパク質結晶解析技術やコンピュータの性能と利用技術の進歩によって，結晶構造が解明されるタンパク質が増加するに伴い，分子の三次元構造（各構成原子の三次元座標で表される構造：立体構造ともいう）を用いた論理的分子設計の重要性が増してきた．特異的に結合するべきタンパク質分子も医薬分子も三次元的存在であることから，三次元構造によってのみ *in vitro* 活性を説明でき，先行化合物の知識なしに新規医薬分子の構造を設計できるはずである．

タンパク質分子の三次元構造として信頼性と精度が高いのは結晶構造である．自社で解析する以外に，プロテインデータバンク（PDB）から三次元座標を入手して利用することができる．そのものずばりのタンパク質の三次元座標が入手できない場合には，同じファミリーのタンパク質の結晶構造を鋳型にしてコンピュータ上で構築したモデリング構造を結晶構造と同様に用いることができる．タンパク質の三次元構造は，基本的な折り畳み構造が大きく変化することは珍しいが，ゆらぎや機能に基づく動きがあり，共存分子や結晶化条件によっても変化する．そのため，標的タンパク質の結晶構造が利用できる場合でも結晶構造は1スナッ

プショットと考えて，リガンドの設計に必要な修正を加えたり，ある程度動きを許容する手立てをしたうえで剛体として利用することが多い．

低分子（リガンド分子）の三次元構造は，原子間の結合距離と結合角と内部回転角によって定義される．これらは実験的には結晶構造解析によって最も精度良く決まるが，論理的分子設計で有用なのは結合距離と結合角である．内部回転角で定義される分子配座は分子の形状を左右することからきわめて重要であるが，問題は低分子の安定配座が置かれた環境により容易に変化しうることである．結晶中の構造と溶液中の構造は異なるし，溶媒によっても，標的タンパク質への結合によっても異なるなど，一般に1個の化学構造が数千個の三次元構造で存在しうる．そこで，医薬分子設計のための計算シミュレーションにおいては，リガンド分子が標的タンパク質と最安定な複合体を形成しうる配座（活性配座）を逃さないために，可能な三次元構造をすべて作り出して試すことが必要になる．

自動ドッキング法に基づく論理的分子設計

われわれは長い間，独自のコンセプトとアルゴリズムに基づいて論理的医薬分子設計のさまざまな方法論を開発してきた．世界に先駆けて開発に成功した方法も多い．さらにそれらの方法を実際の創薬に応用することで，利用のノウハウを蓄積してきた．

標的タンパク質の三次元構造が利用できる場合に最も重要な方法が，任意の分子について標的タンパク質との最安定な複合体構造とその安定性を推定する自動ドッキング法である．ドッキング問題は，両分子の相対的な位置と方向に関する6個の自由度と配座に関する自由度（普通5～10個）によって生じる膨大な数の可能な複合体モデルのなかから，最安定なモデルを実用的な時間内で探索する問題である．複合体モデルの安定性は，タンパク質分子とリガンド分子の原子間でファンデルワールス相互作用，水素結合相互作用，静電相互作用その他からなる力場エネルギーとして評価でき，結晶解析された1個の複合体構造について安定性を計算するだけならパソコンでも容易にできる．

しかし，どんな複合体が形成でされるか全く未知の場合のドッキングスタディでは，すべての可能な複合体モデルについてまともにエネルギーを計算し比較するのは数千倍数万倍の時間がかかり実質的に不可能であった．そこでわれわれは，ドッキングの初期過程において，タンパク質原子を直接用いる代わりに水素結合などの相手となる位置にダミー原子を設定し，その間の距離とリガンド分子中の水素結合原子間の距離を配座を変えながら比較することで，タンパク質分子にはめ込み，有望な複合体モデルを推定できる方法を考案した．

この考案によって世界で初めて配座

の全自由度を考慮した最安定複合体モデルの推定（フレキシブルドッキング）が可能になった．所要時間はペンティアムパソコン上で1分子当たり5～10秒である．安定複合体モデルは，内因性リガンドについては反応や機能が説明でき，先行化合物については構造と活性の関係を説明でき．HTSヒット化合物については結合様式に基づいてリード最適化に進むべき最適化合物の選別ができ，さらに結合様式に基づいて構造修飾の合理的な指針が得られる等々，さまざまな目的にきわめて有用である．

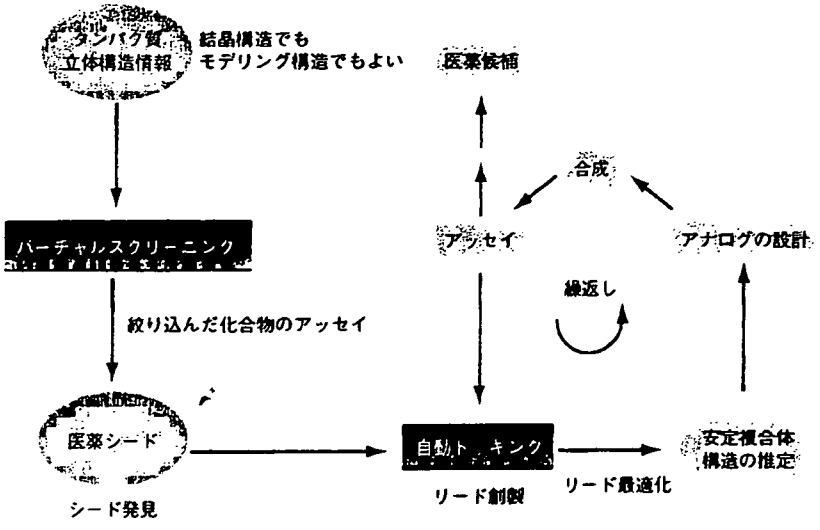

図● IMMDの論理的分子設計に基づく創薬

当社における創薬の流れ．バーチャルスクリーニングを用いて発見した医薬シードを，自動ドッキング法により標的タンパク質との結合様式を推定しつつ設計・合成・アッセイを繰り返すことで論理的に最適化する

バーチャルスクリーニング

既知活性化合物について，標的タンパクとの共結晶化も結晶解析もせずに標的との結合様式や活性配座がわかることも有用であるが，結合するかどうかが未知なだけでなくこの世に存在するかどうかすらわからない化合物について，標的タンパク質との安定な複合体を形成する可能性や安定性を推定できることから，自動ドッキング法は新規リガンドや医薬シード発見に利用できる．すなわち，化合物の三次元構造データベースを用意し，各化合物について自動ドッキングを行って最安定複合体モデルを推定し，その安定性や構造的な特徴があらかじめ設定した基準をクリアーしているか否かによりリガンドとなる可能性の高い少数の有望な化合物を絞り込むバーチャルスクリーニングが可能である．それらの少数の化合物だけを入手（購入または合成）して，目的の活性を測定することにより，新規活性化合物を発見できる．市販化合物のデータベースを対象にすれば，選別した化合物を合成することなく，活性の有無を評価できる．われわれは普通，約30万化合物の市販化合物データベースを対象にバーチャルスクリーニングし，骨格の独立な100個前後の有望な化合物を選別して実験的に評価しているが，そのうち30～40個は新規の活性化合物である．

バーチャルスクリーニングは，①保有していない化合物も対象にできること，②有望な少数に絞り込んで実験するので，丁寧な精度の高いプロファイリングが可能なこと，③結合様式の情報から最適化のための構造修飾の指針が得られること，④低コスト，などの点でHTSより優れている．HTSより不利な点としては，①標的タンパク質の三次元構造情報が必要なこと，②リガンド結合ポケットの特徴や動的挙動について知っておく必要があること，である．われわれはこうして見つけた活性化合物から，構造の薬らしさ，合成の容易さ，結合様式の良さなどを考慮して，1個を出発点として選び，合成展開を行うことで創薬を行っている．われわれがこのアプローチで最初に創薬を行った化合物（IKKβ阻害剤）は，現在P-2a試験に入っており，世界のほとんどの製薬企業が挑戦して失敗したといわれるなかで唯一P-1を終了している“First in the class”である．われわれの創薬の流れを以下の図に示す．

おわりに

創薬は他の開発に比べて格段にお金と時間がかかるうえに，成功する確率よりドロップする確率の方がはるかに

高いハイリスクな研究である．しかし，創薬の後期プロセスである臨床試験の成功が，ヒトと動物の違いや疾患モデルの限界などの容易に超えられない多くの問題に依存するのに対して，初期プロセスである分子設計は科学的な根拠に基づいて論理的に成功率高く効率的に行えるのである．しかし，論理的分子設計は，それらしいことを謳った市販ソフトウェアを買ってきて，その科学的コンセプトの妥当性も限界も考えずにただ計算することで実現できるものではない．われわれは，自ら開発した論理的分子設計法の有用性を証明すべく，いくつかの創薬テーマでその方法を用い有機合成と生化学的評価を組合わせた創薬を実施してきた．次号においてわれわれの創薬の成果について述べる予定である．

水谷実穂（Miho Mizutani）
株式会社医薬分子設計研究所　研究員．
1990年3月東京大学薬学部卒業．1995年3月同大学院薬学系研究科博士課程修了（薬学博士）．1995年4月日本学術振興会特別研究員（PD）．1996年4月社団法人北里研究所研究員．1997年4月より現職．

板井昭子（Akiko Itai）
株式会社医薬分子設計研究所　代表取締役．
1964年3月東京大学薬学部卒業．1969年9月東京大学大学院薬学系研究科博士課程修了（天然物有機化学専攻）．同年10月東京大学薬学部文部教官助手（薬品物理分析学講座）．1990年4月同寄付講座医薬分子設計学講座助教授就任．1994年9月同教授就任．1995年3月株式会社医薬分子設計研究所設立．代表取締役社長として現在に至る．

〈企画：外山　聡・新潟大学医歯学総合病院薬剤部助教授・副薬剤部長〉

論理的分子設計からの創薬

水谷　実穂*1)・板井　昭子*2)

近年，蛋白質の大量産生・精製技術やX線結晶解析技術の進歩により，医薬のターゲットとなる蛋白質の立体構造が数多く解明されてきている。これに伴い，標的蛋白の立体構造に基づく論理的分子設計が，スピーディーで効率的な創薬への重要なアプローチとして注目を集めている。ここでは，ドッキングスタディ，バーチャルスクリーニングを中心とした論理的分子設計のアプローチと，分子レベルでの作用機序を踏まえた医薬開発への寄与について述べる。

Key Words ▶▶ *ドッキングスタディ，バーチャルスクリーニング，蛋白立体構造*

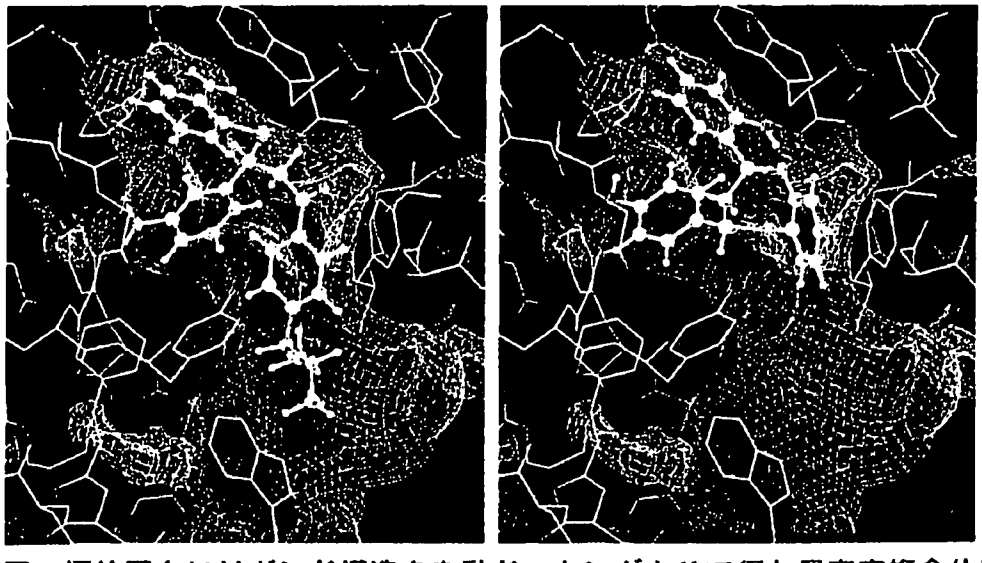

●図　標的蛋白にリガンド構造を自動ドッキングさせて得た最安定複合体モデル（本文図2より）

これらのリガンドは，抗痴呆薬の標的であるアセチルコリンエステラーゼに対し，筆者らのバーチャルスクリーニングを実施して発見された新規阻害薬である．（文献2より）

*株式会社 医薬分子設計研究所　1)（みずたに・みほ）　2) 代表取締役社長（いたい・あきこ）

はじめに

一般に薬物分子は，生体内で標的となる蛋白質（もしくは核酸）と安定な複合体を形成することで，その作用を発現する。図1に示すように，酵素の基質結合部位に結合することにより酵素の働きを阻害したり（抗エイズ薬/HIV〔ヒト免疫不全ウイルス〕蛋白分解酵素の例），核内受容体のリガンド結合部位に結合し，他のドメインやコファクターとの結合に影響を及ぼして転写活性を促進または抑制する（急性前骨髄球性白血病治療薬/レチノイン酸受容体の例）など，さまざまな作用機序があるが，薬物と標

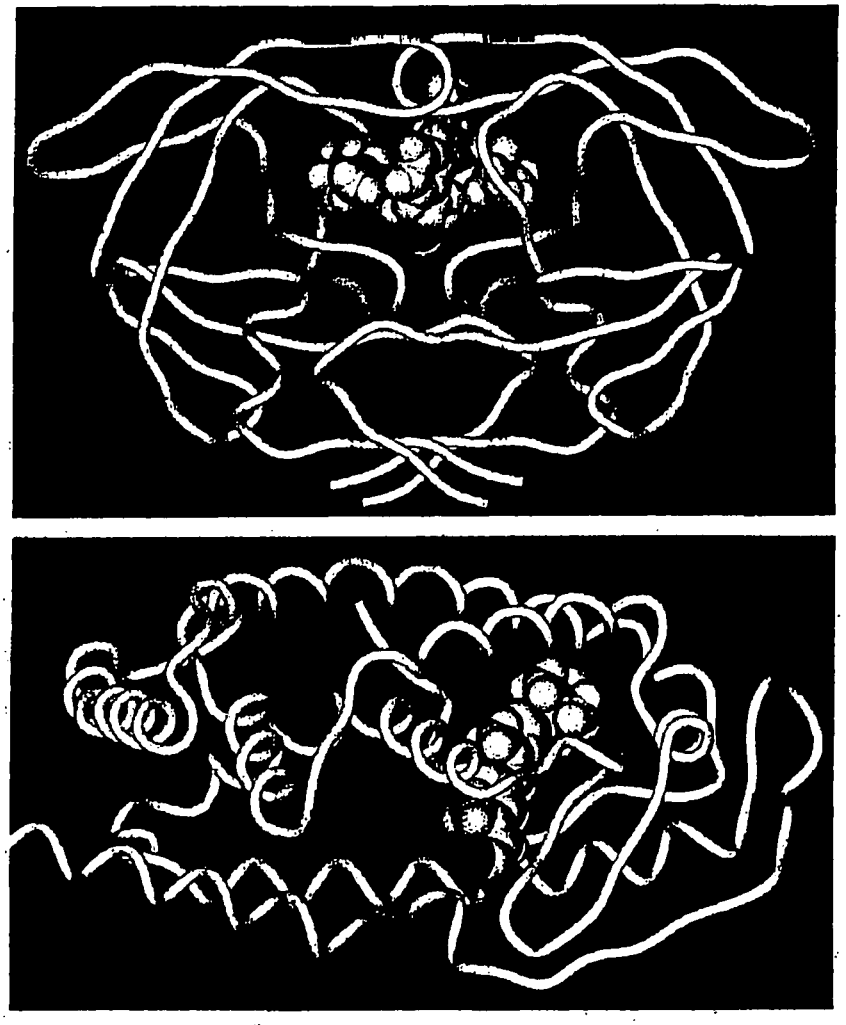

●図1　薬物分子は標的蛋白と安定な複合体を形成する

上：HIV〔ヒト免疫不全ウイルス〕蛋白分解酵素を阻害し，抗エイズ活性を発現するアタザナビル．

下：レチノイン酸受容体に結合し，そのアゴニスト作用によって急性前骨髄球性白血病の治療効果をもたらす全トランス型レチノイン酸．

それぞれ，蛋白質の骨格をチューブで，薬物分子をスペースフィルモデルで示す．

的蛋白が安定な相互作用をするという基本は共通である。

筆者らは，蛋白－薬物相互作用に基づく論理的分子設計の方法論構築に取り組み，またその方法論を利用して実際の創薬にも挑んでいる。本稿では，論理的分子設計の観点から，分子レベルでの作用機序を踏まえた医薬開発について述べてみたい。

蛋白立体構造に基づく論理的分子設計

かつては，既存の薬物や天然物など何らかの薬効を示す活性化合物を，作用機序等は分からないままに出発点として，医薬開発を行ってきた。開発のスタート時に作用機序や標的蛋白を設定するようになったのは，ここ10年余りのことである。現在は，蛋白質の大量産生・精製技術やX線結晶解析技術の進歩により，医薬のターゲットとなる蛋白質の立体構造が数多く解明されてきている。論理的分子設計は，標的蛋白の立体構造を利用して，薬物などのリガンドが結合する蛋白ポケットに，形状や静電的な性質がよくフィットし，特異的な相互作用(水素結合など)を形成し得る多様な低分子構造を提示できる手法である。効率的でスピーディーな創薬の成功をもたらすアプローチとして期待を集めている。

ドッキングスタディの重要性

ドッキングスタディとは，標的蛋白と任意の低分子化合物とで形成される安定な複合体構造を推定する，分子設計の手法である。標的蛋白の立体構造は，結晶構造に限らず蛋白モデリング法により構築したものでもよい。ドッキングによって推定した最安定な複合体構造モデルから，蛋白に結合した時のリガンドのコンフォメーションや，分子間の水素結合など特異的な相互作用の様子を知ることができる。(図2)。最安定複合体モデルとその安定性（エネルギー値）からは，実に多くの情報や示唆が得られる。例えば，① 薬物や活性化合物の分子レベルでの作用機序を推定するのに役立つ，② 一連の活性化合物の結合様式や安定性を比較することで，化合物の構造と活性の相関関係（構造活性相関）を説明できる，③ 活性化合物を複数有している場合，そのいずれを合成展開の出発化合物とするか，選択のための重要な判断材料が得られる，④ 結合様式から，活性や動態，物性を向上させるための指針が得られる，などである。また，標的蛋白の類縁蛋白質への結合の様式や安定性を検討することで，リガンドの選択性を向上させたり（図3），薬剤耐性を獲得した変異蛋白をターゲットとした薬物設計を行うことも可能である。

自動ドッキング法からバーチャルスクリーニングへ

ドッキングスタディは論理的薬物設計において中心的なアプローチであるが，これを研究者が手作業で行うのは難しい。正しい複合体構造モデルを得るためには，化合物のコンフォメーションの自由度も考慮しながら，蛋白－化合物間の相対配置の可能性を漏れなく探索する必要がある。ところが，ここで考慮すべき可能性の数は恐ろしく膨大であり，人間が網羅探索することは考えられない。そこで，筆者らはそれらの可能性について，コンピュータを用いて自動的かつ効率的に網羅探索する手法を，世界に先駆けて考案した[1]。

筆者らはさらに，この自動ドッキング法をバーチャルスクリーニング法へと発展させた[2]。バーチャルスクリーニング法は，数十万～数百万分子を収めた化合物構造データベースから，標的蛋白に安定に

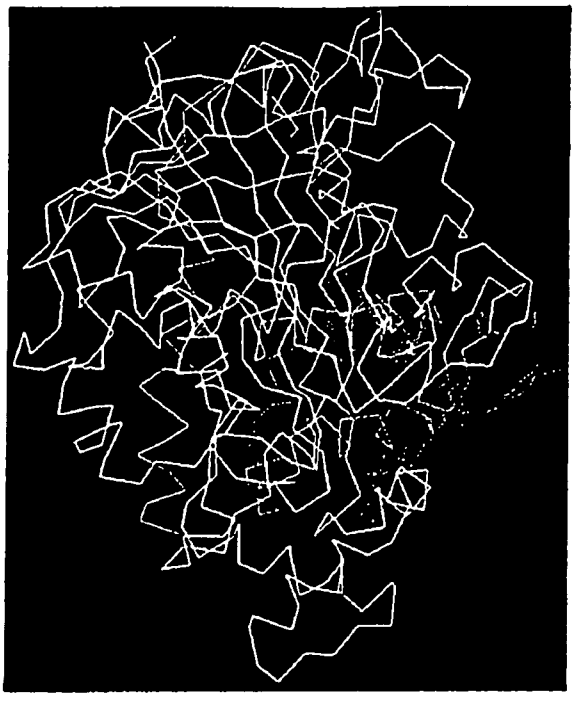

a

b | c

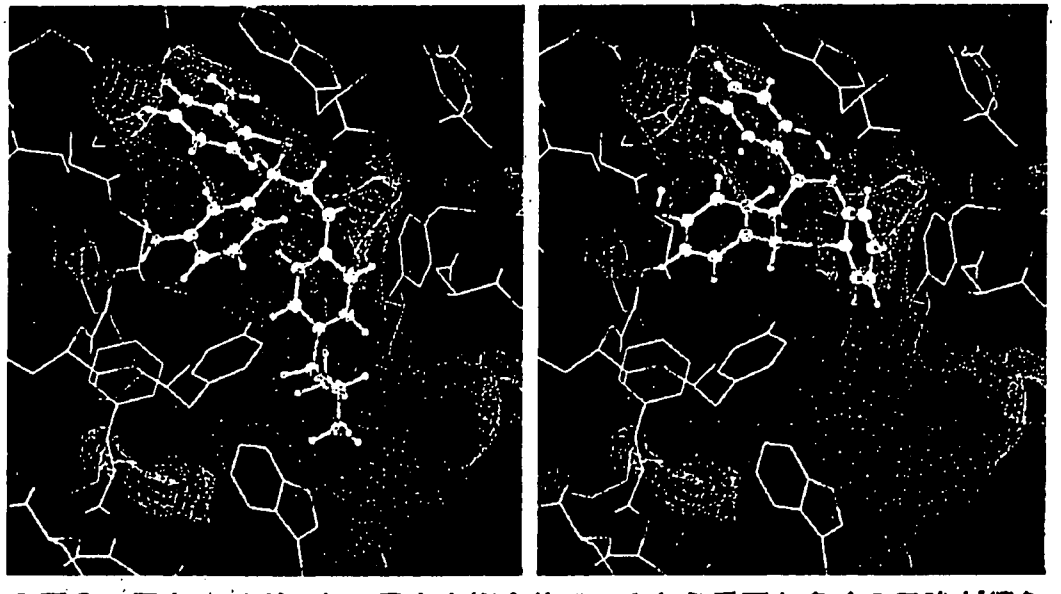

●図２　蛋白ーリガンドの最安定複合体モデルから重要な多くの示唆が得られる（再掲）

ａ：標的蛋白のリガンド結合キャビティ（カゴ状の領域）．蛋白構造はＣαのみ表示．

ｂ，ｃ：標的蛋白にリガンド構造を自動ドッキングさせて得た最安定複合体モデル．

これらのリガンドは，抗痴呆薬の標的であるアセチルコリンエステラーゼに対し，筆者らのバーチャルスクリーニングを実施して発見された新規阻害剤である．

推定結合様式をもとに，合成展開の出発化合物を選択したり，展開の指針を得ることができる．

（文献２より）